



CHALMERS
UNIVERSITY OF TECHNOLOGY

Thermal stability of low and high Mw fractions of bio-oil derived from lignin conversion in subcritical water

Downloaded from: <https://research.chalmers.se>, 2024-04-25 05:11 UTC

Citation for the original published paper (version of record):

Nguyen Lyckeskog, H., Mattsson, C., Olausson, L. et al (2017). Thermal stability of low and high Mw fractions of bio-oil derived from lignin conversion in subcritical water. *Biomass Conversion and Biorefinery*, 7(4): 401-414.
<http://dx.doi.org/10.1007/s13399-016-0228-4>

N.B. When citing this work, cite the original published paper.

Thermal stability of low and high Mw fractions of bio-oil derived from lignin conversion in subcritical water

Huyen Nguyen Lyckeskog¹ · Cecilia Mattsson¹ · Lars Olausson² ·
Sven-Ingvar Andersson¹ · Lennart Vamling¹ · Hans Theliander¹

Received: 13 September 2016 / Revised: 10 November 2016 / Accepted: 21 November 2016 / Published online: 21 December 2016
© The Author(s) 2016. This article is published with open access at Springerlink.com

Abstract The thermal stability of bio-oil influences its application in industry and is, therefore, a very important factor that must be taken into consideration. In this study, the stability of low and high molecular weight (Mw) fractions of bio-oil obtained from the hydrothermal liquefaction (HTL) of lignin in subcritical water was studied at an elevated temperature (80 °C) for a period of 1 h, 1 day and 1 week. The changes in molecular weight (gel permeation chromatography (GPC)) and chemical composition (gas chromatography–mass spectrometry (GC–MS) and 2D heteronuclear single quantum correlation (HSQC) NMR (18.8 T, DMSO- d_6)) of low and high Mw fractions of the HTL bio-oil (i.e. light oil (LO) and heavy oil (HO)) were evaluated before and after ageing. It was found that only a slight formation of high Mw insoluble structures

was obtained during ageing at elevated temperature for 1 week: 0.5% for the LO and 3.1% for the HO. These higher Mw moieties might be formed from different polymerisation/condensation reactions of the reactive compounds (i.e. anisoles, guaiacols, phenols, methylene ($-CH_2-$) groups in phenolic dimers and xanthene). The high Mw insolubles in both the LO and the HO were analysed for structural composition using 2D HSQC NMR to obtain a better understanding of the changes in the composition of bio-oil fractions during the accelerated ageing process. In addition, a chemical shift database in DMSO- d_6 was analysed for a subset of phenolic model compounds to simplify the interpretation of the 2D HSQC NMR spectra.

Keywords Lignin · Bio-oil · Hydrothermal liquefaction · Subcritical water · Stability · Storage

Electronic supplementary material The online version of this article (doi:10.1007/s13399-016-0228-4) contains supplementary material, which is available to authorized users.

✉ Hans Theliander
hanst@chalmers.se

Huyen Nguyen Lyckeskog
huyen@chalmers.se

Cecilia Mattsson
cecilia.mattsson@chalmers.se

Lars Olausson
lars.olausson@chalmers.se

Sven-Ingvar Andersson
sianders@chalmers.se

Lennart Vamling
lennart.vamling@chalmers.se

1 Introduction

It is of the utmost importance that a bio-oil has a low reactivity so that it may retain its properties during storage and shipping. Although relatively few studies can be found in the literature regarding the stability of bio-oil during storage, and particularly at elevated temperatures, there are some regarding bio-oil produced from biomass-pyrolysis [1]. However, the biomass-pyrolysis bio-oil has high contents of water (20–30%), oxygen (45–60%) and acid (pH 2.0–4.0), which make it thermally and chemically unstable [2]. Biomass-pyrolysis bio-oil is composed of a wide range of compounds (including acids, phenols, aldehydes, ketones and oxygenated compounds) that may react and form larger molecules during storage [3]. A huge number of possible reactions may occur, with one important type being oxidative degradation [2]. This causes superoxide to form which, in turn, catalyses polymerisation and

¹ Department of Chemistry and Chemical Engineering, Chalmers University of Technology, SE-412 96 Gothenburg, Sweden

² Valmet Power AB, Box 8734, SE-402 75 Gothenburg, Sweden

results in an increase in molecular weight and viscosity. Another type of reaction is thermal degradation (at elevated temperature), which may lead to the decomposition of components and thus result in the loss of volatiles or an increase in viscosity [2]. These generate challenges in the handling, transportation, storage and use of bio-oil as a fuel [4, 5]. In order to increase the stability of bio-oil, various methods (chemical and physical) have been proposed. The main concept behind them is to reduce reactivity and acidity (by the addition of solvent/antioxidant, emulsification or drying the biomass) or to remove the solid char/ash content (by filtering the bio-oil or treating the biomass) of the bio-oil. Metal ions (e.g. potassium, sodium, calcium and magnesium) retained in ash/char act as catalysts, activating condensation reactions in the bio-oil. Consequently, removing these particular solid chars/ashes is vital in reducing the ageing process of bio-oil [2, 5].

As far as thermal stability is concerned, a few studies on the chemical changes of biomass-pyrolysis bio-oil stored at elevated temperatures (up to 90 °C) over extended periods of time (up to 1 week) using different methodology can be found in the literature [3, 4, 6–12]. Boucher et al. [7], Hilten et al. [3] and Samanya et al. [8] argued that 80 °C was a suitable temperature for testing thermal stability since, at this temperature, rather large change in the properties of biomass-pyrolysis bio-oil can be expected. The amount of insolubles in biomass-pyrolysis bio-oil was found to increase considerably during accelerating ageing at elevated temperature (i.e. 0.5–26%) in various studies [1, 7, 13–15]. Further important properties to study are the variations in the chemical structural changes (gas chromatography–mass spectrometry (GC–MS) and nuclear magnetic resonance (NMR)) and the molecular weight (Mw) during ageing. It has also been shown to be very beneficial to apply a fractionation approach when studying reaction mechanisms and chemical structural changes in bio-oil because it is much more representative of the actual reaction environments than model compounds [11]. According to these authors, the water-insoluble fraction (pyrolytic lignin fraction) showed a significant increase in Mw after accelerated ageing at 80 °C and that a higher increase was obtained with a higher ageing temperature (110 °C). They also reported that the accelerated process gave an increase in aromatic C–O and C–C bonds and a decrease in aromatic C–H and aliphatic C–O bonds in the pyrolysis bio-oil through lignin condensation. In another study, Meng et al. [14] reported that there was an increase in alkyl carbons (about 9.5%) and aromatic carbons (about 16.1%) but a decrease in methoxyl carbons (about 12.3%) when the biomass-pyrolysis bio-oil was aged at 80 °C for 24 h. Consequently, all of the condensation reactions in the biomass-pyrolysis bio-oil consume methoxyl groups and form new aromatic C–C, thus increasing the Mw of the bio-oil components during ageing. This is in agreement with the results of Garcia-Pérez et al. [13] and Chaala et al. [16] obtained in ageing studies of biomass-pyrolysis bio-oil. These authors

revealed that the ageing reactions (polycondensation/polymerisation) in the biomass-pyrolysis bio-oil formed the high Mw compounds from polyaromatic compounds that contributed to the formation of tridimensional network structures. In a recent review relating to the multiphase nature of biomass-pyrolysis bio-oil [17], Oasmaa et al. reported that phase separation occurred during ageing due to the reduction of light Mw fraction, together with the formation of extra water and water insoluble heavy Mw fraction.

Based on the chemical changes that occur in biomass-pyrolysis bio-oil, different ageing pathways have been proposed. One plausible ageing mechanism of the polymerisation/condensation reactions in the biomass-pyrolysis bio-oil is the acid-catalysed reactions between the electron-rich aromatic ring and the cationic sites provided by benzyl alcohol and benzyl ether at the α -carbon [14]; another is the radical reactions that could take place under an acid-free condition. These reactions are based on the aromatic substrate substitutions involving the coupling of the aromatic rings from the aromatic free radicals. These free radicals may be produced either by bond cleavage in the HTL process or the stereo-electronic effect of aromatic rings [10, 18]. They then attack the other rings, leading the formation of a higher Mw compounds (i.e. the condensed products) [19].

Another type of bio-oil is obtained from the catalytic conversion/HTL of lignin under subcritical water conditions. In a recent study of Nguyen Lyckeskog et al. [20], the storage stability of this HTL bio-oil was investigated at ambient temperature for a period of 2 years. The HTL bio-oil was found to retain high degree of storage stability, especially the low Mw fraction (LO, a diethyl ether soluble fraction). The properties of this type of bio-oil are quite different to those of bio-oil obtained by pyrolysis, which may explain the relatively high stability at ambient temperature: it has low contents of both oxygen (15–21%) and water (11–19%). Moreover, the active organic functional groups in HTL bio-oil are different to those found in pyrolysis bio-oil: the major constituents in the former are phenolic aromatics, i.e. substituted with hydroxyl, methoxyl and alkyl groups, and only a small amount of carboxylic acids/aldehydes groups are to be found. It was shown that these active organic functional groups combine with residues of ash and influence the stability of the HTL bio-oil negatively [20–24]. The complexity of the chemical composition of bio-oil has meant that studies on the ageing of HTL bio-oil at a molecular level have rarely been published, particularly with respect to the ageing of lignin derived HTL bio-oil.

To the best of the authors' knowledge, no systematic study on the ageing at elevated temperatures of lignin-derived bio-oil products obtained from HTL has been published in a scientific journal so far. The aim of the present work was to study the ageing behaviour of isolated bio-oil fractions during the accelerated ageing process. These bio-oil fractions (i.e. LO and HO) were aged at an elevated temperature of 80 °C at

various residence times (i.e. 1 h, 1 day and 1 week). The changes in molecular weight and chemical composition were investigated before and after ageing using gel permeation chromatography (GPC), GC–MS and high resolution 2D heteronuclear single quantum correlation (HSQC) NMR (800 MHz).

2 Materials and methods

2.1 Production of the bio-oil

The samples of bio-oil investigated in this work came from a process in which LignoBoost Kraft softwood lignin was converted into bio-oil in a continuous reactor operating at subcritical conditions in water; the samples are characterised elsewhere [20–24]. In these experiments, the reactor temperature and pressure were kept at 350 °C and 25 MPa, respectively. In the feed, the dry lignin content was about 5.6% and the mass ratio of phenol to dry lignin was 0.70, whilst the concentrations of K₂CO₃ and KOH were 1.6 and 0.4%, respectively. The heterogeneous catalyst used in this process was zirconia (ZrO₂) manufactured by Saint-Gobain Norpro, USA. The flow rate of the feed was 2 kg/h, the recycle-to-feed ratio was 4 and the steady-state period for sampling was 1 h and 20 min. Further details of the apparatus and procedure related to the production of lignin-derived bio-oil can be found in previous work by Nguyen et al. [21, 22] and Belkheiri et al. [23, 24].

2.2 Fractionation of the bio-oil

In order to distinguish the different fractions, a work procedure was developed to separate the lignin-derived bio-oil into LO (the low Mw fraction) and HO (the high Mw fraction) using diethyl ether (DEE) and tetrahydrofuran (THF). A block diagram describing the various steps of the fractionation procedure is shown in Fig. 1. The bio-oil was first extracted using DEE, with a solvent-to-feed ratio (S/F) of 20/1 and then separated into two fractions: one DEE-solubles (LO) and the other DEE-insolubles. The DEE-insoluble fraction was further extracted using THF, with S/F ratio of 20/1, into two fractions: one THF-solubles (HO) and the other THF-insolubles. In this study, the bio-oil sample obtained from the HTL lignin conversion was fractionated and gave a yield of 69.8% LO, 12.7% HO and 17.5% THF insolubles. The mass balance was closed by the masses measured for the DEE and THF insoluble (Eqs. S1–3). Further details regarding the bio-oil fractionation has been reported previously in Nguyen Lyckeskog et al. [20].

2.3 Accelerated ageing of the bio-oil

The bio-oil fractions (LO and HO) were subjected to accelerated ageing at a temperature of 80 °C for various periods of

time (1 h, 1 day and 1 week). The stability test was performed according to Elliott et al. [25]. About 2.5 g LO and 0.5 g HO were poured into 10-mL Schott Duran bottles (with screw caps) and placed in a heating oven at 80 °C. After ageing, the LO was fractionated into DEE-solubles and DEE-insolubles (aLO_ES_80 and aLO_EIS_80), and the HO was fractionated into THF-solubles and THF-insolubles (aHO_TS_80 and aHO_TIS_80) (see Fig. 1). Also, about 0.3 g LO were put into Schott Duran bottles and used for GC–MS analysis after undergoing accelerated ageing at 80 °C for different periods of time.

2.4 Characterisation of the bio-oil

2.4.1 Molecular weight of light oil, heavy oil and THF insolubles (GPC analysis)

About 30 mg of each sample (fresh LO, aged LO_DEE solubles/insolubles (aLO_ES/EIS_80), fresh HO, aged HO_THF solubles/insolubles (aHO_TS/TIS_80) and fresh THF insolubles (TIS)) were dissolved in the mobile phase of dimethyl sulphoxide and LiBr (DMSO/LiBr 10 mM) and then filtered with a 0.2-µm syringe filter. The molecular weight (Mw) and molecular weight distribution (MwD) of these samples were analysed using gel permeation chromatography (PL-GPC 50 plus) connected to refractive index (RI) and ultraviolet (UV) detectors (280 nm, Polymer Laboratories, Varian Inc.). Two PolarGel-M columns and a guard column (300 × 7.5 and 50 × 7.5 mm, 8 µm) are coupled in series. A 10-point calibration curve with Pullulan standards (polysaccharide calibrations kit, PL2090-0100, Varian) was used to determine the Mw of the samples. The samples were analysed in triplicate and the average value was employed. All the samples in this study were found to be soluble in the mobile phase (DMSO/LiBr). By using DMSO/LiBr as mobile phase, all bio-oil fractions Mw could be compared to the starting material without acetylation of the samples.

2.4.2 Chemical composition of light oil (GC–MS analysis)

GC–MS was used to determine the chemical composition of the samples (LO, aLO_ES_80). About 0.3 g of samples was dissolved in DEE with an S/F of 30 and mixed with a known amount of internal standard IST (syringol in DEE). This mixture was filtered through a 0.2-µm syringe filter and injected into the GC–MS system. The gas chromatography (GC, Agilent 7890A) used was coupled with mass spectrometry (MS, Agilent 5975C) operating in electron ionisation mode. The analytes were separated in a chromatographic column HP-5MS (length 30 m, internal diameter 0.25 mm, thickness of stationary phase 0.25 µm) by injecting in 1 µL of sample with a split ratio of 10 via an auto-sampler (Agilent 7693A), using helium at 1 mL/min as the carrier gas. The injector

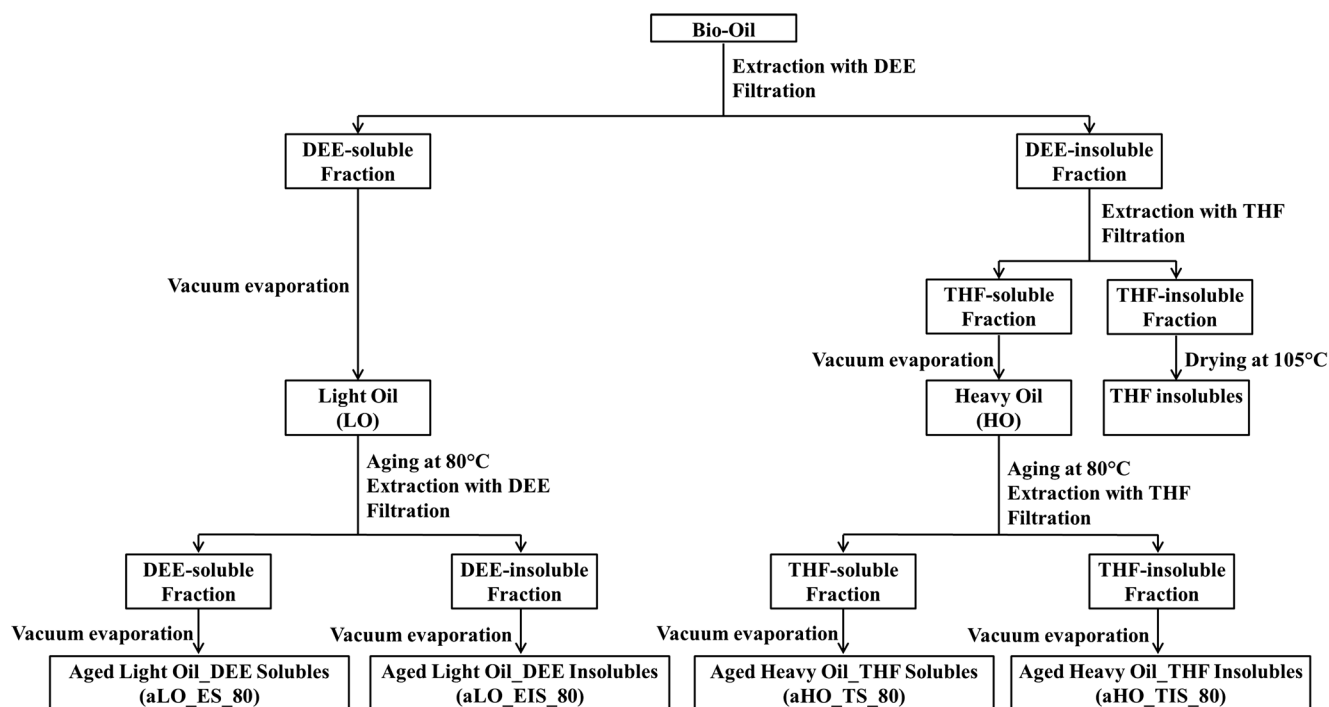


Fig. 1 Block diagram of the solvent fractionation of the lignin-derived HTL bio-oil at fresh and aged states. DEE diethyl ether, THF tetrahydrofuran

temperature was set at 300 °C and the temperature programme of the GC oven was 45 °C for 2.25 min, 2 °C/min up to 300 °C and then 300 °C for 10 min. The MS source and quadrupole temperatures were set at 250 and 150 °C, respectively. Spectral interpretation was carried out using the NIST MS Search Programme (version 2.0) operating on the NIST/EPA/NIH Mass Spectral Database 2011 (NIST 11). The content of the main components were determined semi-quantitatively; each sample was analysed in triplicate and the average value was employed.

2.4.3 Functional groups of light oil, heavy oil and THF insolubles (2D HSQC NMR analysis)

Here, the samples (LO, aLO_ES/EIS_80, aHO_TS/TIS_80 and TIS) were dissolved in the dimethyl sulphoxide- d_6 (DMSO- d_6) for NMR analysis. About 100 mg of samples (LO, aLO_ES_80, HO, aHO_TS_80, TIS) was dissolved in 0.75 mL DMSO- d_6 through a small vial equipped with a stirring bar; they were mixed overnight to ensure complete dissolution. However, due to the small amount of insoluble fractions was obtained after ageing, only about 10–35 mg of these fractions samples (aLO_EIS_80, aHO_TIS_80) were dissolved in 0.25 mL DMSO- d_6 . The sample solutions were analysed by means of ^1H - ^{13}C HSQC NMR (Bruker, 800 MHz). The correlation spectra were recorded at 25 °C on a Bruker Advance III HD 18.8 T NMR spectrometers (Rheinstetten, Germany) equipped with a 5-mm TXO cryoprobe (for 100 mg sample/0.75 mL DMSO- d_6 solutions) and a 3-mm TCI cryoprobe (for 10–35 mg sample/0.25 mL DMSO-

d_6 solutions). The HSQC spectra were recorded with a standard Bruker pulse sequence “hsqcedetgpsisp2.3”, 0.25 s ^1H acquisition time, 5.3 ms ^{13}C acquisition time, 3 s interscan delay, 1JC–H coupling constant of 145 Hz, 8 scans (for 100 mg sample/0.75 mL DMSO- d_6 solutions) and 16–48 scans (for 10–35 mg sample/0.25 mL DMSO- d_6 solutions). The spectrum was recorded for 4 h (for 100 mg sample/0.75 mL DMSO- d_6 solutions) and up to 16 h (for 10–35 mg sample/0.25 mL DMSO- d_6 solutions). The spectra were processed and analysed using MestReNova v10.0.0 software’s default processing template and automatic phase and baseline correction. Besides, the HSQC spectra for the model compounds were recorded with 20% NUS with 21 ms ^{13}C acquisition time, four scans, 2 s relaxation delay and total measurement time of 1 h. The spectra were processed using MDDNMR software.

3 Results

3.1 Fractionation and yields of the bio-oil

Following accelerated ageing of the LO and HO at 80 °C for different periods of time (1 h, 1 day and 1 week), as described above, the LO and HO were fractionated using DEE and THF, respectively; Table 1 shows the yield of each fraction obtained. No significant change in the yields of LO and HO was observed when they were aged at 80 °C for up to 1 day. A slight decrease in yields was, however, found after accelerated ageing at 80 °C for 1 week: from 100 to 99.5% for the LO and

Table 1 Yields (%) of the aged light oil_DEE solubles (aLO_ES_80) and aged heavy oil_THF solubles (aHO_TS_80), calculated by the mass measured for the DEE insolubles on the dry basis, at different ageing times compared to the fresh state^a

Ageing time	Aged light oil_DEE solubles (aLO_ES_80)	Aged heavy oil_THF solubles (aHO_TS_80)
Fresh	100.0	100.0
1 h	100.0	100.0
1 day	99.9	99.7
1 week	99.5	96.9

^a The RSD was about 0.2% for the light oil and 2.2% for the heavy oil

from 100 to 96.9% for the HO. This indicates that not only the LO but also the HO are quite stable at 80 °C.

An image of the mixture of LO (after ageing at 80 °C for different periods of time) and DEE is shown in Fig. 2. As can be seen that although a trace amount of insoluble fraction was formed in the aged LO (aLO_EIS_80) after 1 h of ageing, the amount of DEE insolubles (aLO_EIS_80) obtained increased after 1 week of ageing. The same trend could also be observed for the THF insolubles obtained in the aged HO (aHO_TIS_80), but with a higher rate of formation (not shown in Fig. 2). The formation of insolubles (aLO_EIS_80 and aHO_TIS_80) explains the decrease in yields of the LO and HO after ageing (Table 1). The yield of insolubles in the aged LO (aLO_EIS_80) and the aged HO (aHO_TIS_80) after 1 week of ageing is 0.5 and 3.1%, respectively, showing that the ageing rate of HO is faster than that of LO at 80 °C for 1 week. The formation rate of insolubles (aLO_EIS_80 and aHO_TIS_80) in this study is relatively low compared to the biomass-pyrolysis bio-oil [1, 7, 13–15]. The LO and HO produced by the HTL of lignin have, thus, a comparably high degree of stability at 80 °C.

3.2 Determination of the molecular weight of lignin-derived bio-oil fractions

It should be noted that the retention time determined by GPC depends not only on the molecular size of the molecule but also on the functional groups present: it is preferable that the

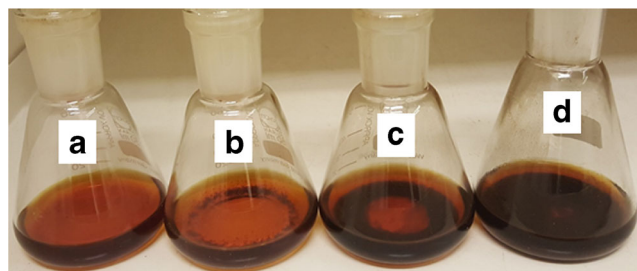


Fig. 2 Light oil mixed with DEE at S/F of 30: fresh state (a); aged states at 80 °C for 1 h (b), for 1 day (c) and for 1 week (d)

standards used for the calibration curves possess the same functional groups as the compounds to be analysed. The lignin-derived bio-oil, however, consists of a complex mixture of various compounds containing a large number of different functional groups, which makes it impossible, in practice, to have suitable GPC standards here. There may, therefore, be a systematic deviation in the Mw that is determined: since the methodology is the same for all of the samples, however, it is possible to make comparisons. The MwD curves of LO, HO and THF insolubles at fresh state (LO, HO and TIS) are shown in Fig. 3. The Mw increases in the order of LO, HO and THF insolubles. The LO comprises a high amount of monomers (peak 1, ~60 Da) and a low amount of dimers (peak 2, ~250 Da) and oligomers (peak 3, ~2500 Da). The HO comprises mainly oligomers, with a low amount of peak 3 and a higher amount of peak 4 (~5600 Da). The THF insolubles have just one peak, with high Mw oligomers (peak 5, ~17,000 Da).

The MwD curves of the fresh LO, aged LO_DEE solubles (aLO_ES_80_1h/1d/1w) and aged LO_DEE insolubles (aLO_EIS_80_1h/1d/1w) are presented in Fig. 4a. As can be seen, the curves for the fresh LO and the aged LO_DEE solubles at different ageing times are almost identical: no increase in Mw can be detected. The aged LO_DEE insolubles that were formed were found to have a molecular weight of about 6000 Da, and it was independent of ageing time. Furthermore, these insolubles (~6000 Da) were found to be in the same Mw range as the fresh HO (~5600 Da). The MwD curves for the fresh HO, aged HO_THF solubles (aHO_TS_80_1h/1d/1w) and aged HO_THF insolubles (aHO_TIS_80_1d/1w) are shown in Fig. 4b. Similar to the LO, the MwD curves for the fresh HO and aged HO_THF solubles at different ageing times are almost indistinguishable (Mw ~5600 Da). The aged HO_THF insolubles that were formed were found to have a molecular weight of about 11,000 Da, which is significantly lower than the THF insolubles found in the fresh bio-oil (TIS, ~17,000 Da). The materials with a high Mw in the bio-oil have thus become larger after ageing, indicating that the materials with a low Mw have been polymerised and now have a high Mw.

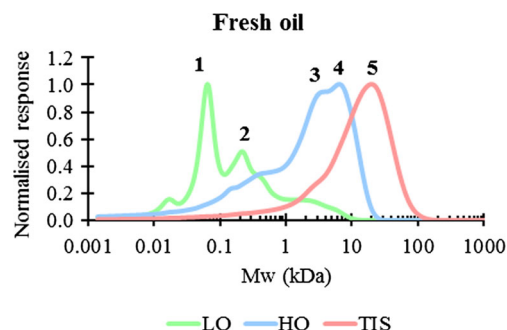


Fig. 3 MwD curves for the fresh bio-oil: light oil (LO), heavy oil (HO) and THF insolubles (TIS)

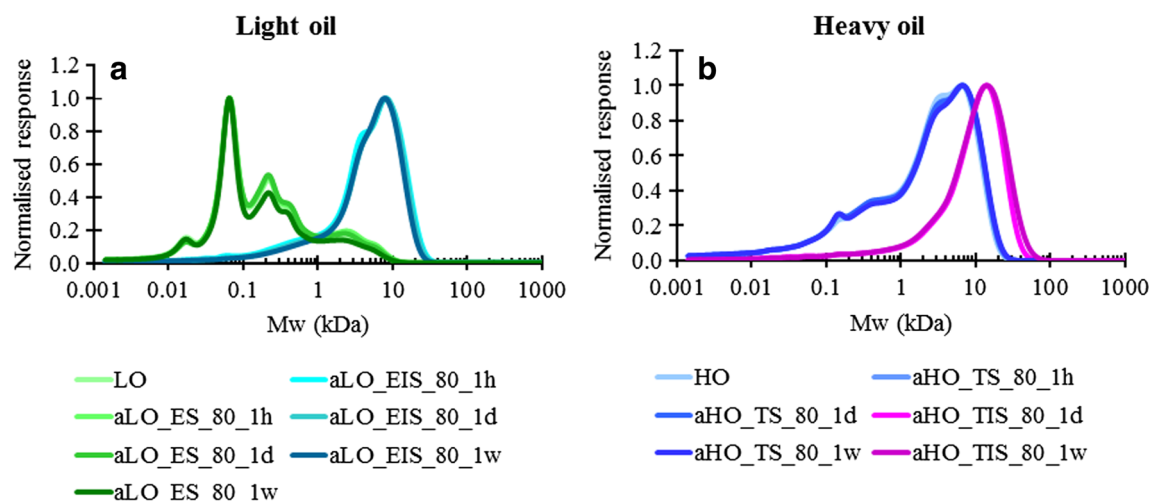


Fig. 4 MwD curves for **a** the fresh light oil (LO) and aged light oil at 80 °C (aLO_ES/EIS_80) and **b** the fresh heavy oil (HO) and aged heavy oil at 80 °C (aHO_TS/TIS_80)

3.3 Light oil

3.3.1 GC–MS analysis

GC–MS analysis of the DEE solubles in the bio-oil at fresh and aged states was performed to identify and quantify the amount of major monomeric aromatics present in these fractions, which corresponded to about 30% of the original bio-oil. Table 2 shows detailed data for the yield of the compounds that were identified on a dry basis. The compounds were classified based on structure, e.g. phenols (phenol and alkyl phenols), anisoles (anisole and alkyl anisoles), guaiacols (guaiacol and alkyl guaiacols) and catechols (catechol and alkyl catechols) to gain a better understanding of the effects that ageing has on the distribution of monomeric aromatics.

In general, no large changes in the yield of small aromatics could be detected after accelerated ageing at 80 °C for up to 1 day. However, after ageing for 1 week, small changes in yield could be observed. The most reactive classes of compounds were found to be in the order: xanthene > anisoles >> guaiacols, phenols, phenolic dimers (Ar–CH₂–Ar, methylene bridge) >>> catechol, phenolic dimers (Ar–CH₂–CH₂–Ar, ethylene bridge). In particular, there was a decrease in the yield of xanthene, anisoles, guaiacols, phenols and phenolic dimers (methylene –CH₂– group) of about 87, 36, 13, 10 and 8%, respectively, after 1 week of ageing at 80 °C, and it is consistent with the yield results given in Table 1. This reveals the different sensitivity of the functional groups found in the lignin-derived bio-oil.

The findings that the decrease in anisoles and guaiacols was higher than in phenols and phenolic dimers (Ar–CH₂–Ar) indicate that aromatic rings attached with the methoxyl groups (–OCH₃) are more reactive than the corresponding ones with the hydroxyl groups (–OH) in the bio-oil. This is in agreement with the results obtained by Ben and Ragauskas [26], who reported that the bond energy of the C–O bond

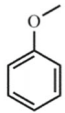
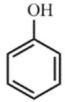
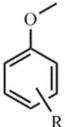
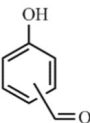
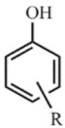
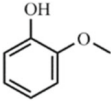
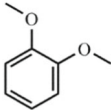
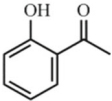
(CH₃–O) in the methoxyl groups is lower than the O–H bond in the hydroxyl groups, which shows that the methoxyl groups decompose more easily than the hydroxyl groups.

Furthermore, the ethylene group (–CH₂–CH₂–) between two aromatic rings was found more stable than the methylene (–CH₂–) group in the bio-oil. This is consistent with the work of Johns et al. [27], who concluded that the relative stability of bibenzyl (Ar–CH₂–CH₂–Ar) is higher than that of diphenylmethane (Ar–CH₂–Ar). Moreover, xanthene having the methylene (–CH₂–) group also showed a high reactivity. The stereo-electronic effect causes the C–H bond in the methylene –CH₂– group between two aromatic rings of phenolic dimers and xanthene weaken synergistically, which makes the structure of phenolic dimers (Ar–CH₂–Ar) and xanthene unstable and thus vulnerable to be attacked by a nucleophile for electrophilic substitution [28]. Besides, these structures (phenolic dimers with methylene groups and xanthene) have a high number of non-substituted *o*–/*p*– sites (i.e. free *o*–/*p*–carbons) which may participate in the additional condensation reactions during the accelerated ageing [29].

In addition, catechols showed a low reactivity in this study. This is supported by Joseph et al. [1], who found catechols to have a reduced reactivity in model studies at 80 °C for a period time of 40 h. A reduced activity of catechol rings can be ascribed to the lack of ring activation due to counteracting effects when two hydroxyl groups are substituted in a 1,2-pattern. Also, retene (or 7-isopropyl-1-methyl phenanthrene) was found to be relatively stable. Retene is a polycyclic aromatic hydrocarbon (PAH), a class of compounds that are comprised of neither methoxyl (–OCH₃) group nor hydroxyl (–OH) group on the aromatic rings. This kind of compound is thermally stable: a very high temperature (800 °C) is required for its thermal decomposition or for condensation to occur [30].

Consequently, a few different structural motifs, e.g. methoxyl groups and methylene bridges between aromatic

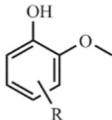
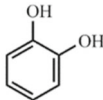
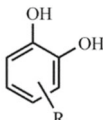
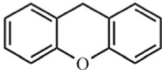
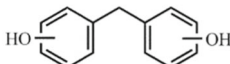
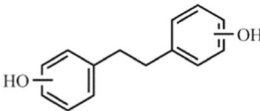
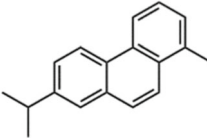
Table 2 Yields (%) of GC–MS compounds identified in the fresh light oil (LO) and aged light oil_DEE solubles (aLO_ES_80) on a dry basis

Compounds	Structures ^a	LO	aLO_ES_80_1h	aLO_ES_80_1d	aLO_ES_80_1w
Anisole		9.24	8.99	8.07	5.84
Phenol		20.00	20.14	19.45	18.00
Alkyl anisoles		1.02	0.99	0.87	0.65
Hydroxy-benzaldehyde		0.11	0.11	0.11	0.10
Alkyl phenols		5.49	5.51	5.30	4.90
Guaiacol		2.54	2.54	2.44	2.20
1,2-Dimethoxybenzene		0.20	0.20	0.20	0.18
2-Acetylphenol		0.26	0.26	0.24	0.22

rings (Ar–CH₂–Ar, xanthene), were found to have high reactivity, whereas other structural combinations, such as catechols, ethylene bridges between aromatic rings (Ar–CH₂–CH₂–Ar) and PAH-like structures (retene), were found to be

more stable. These findings are consistent with the literature data on the stability of pure compounds at ambient temperature with the order: anisoles > guaiacols > phenols > catechols > phenolic dimers [31–35].

Table 2 (continued)

Alkyl guaiacols		0.89	0.90	0.85	0.78
Catechol		0.16	0.16	0.15	0.18
Alkyl catechols		0.25	0.24	0.21	0.22
Xanthene		0.38	0.38	0.20	0.05
Phenolic dimers (Ar-CH ₂ -Ar)		3.03	3.04	2.91	2.78
Phenolic dimers (Ar-CH ₂ -CH ₂ -Ar)		0.71	0.71	0.66	0.67
Retene		0.13	0.12	0.13	0.13
Total excluding phenol		24.4	24.2	22.3	18.9

^aR is the alkyl group attached to the aromatic ring

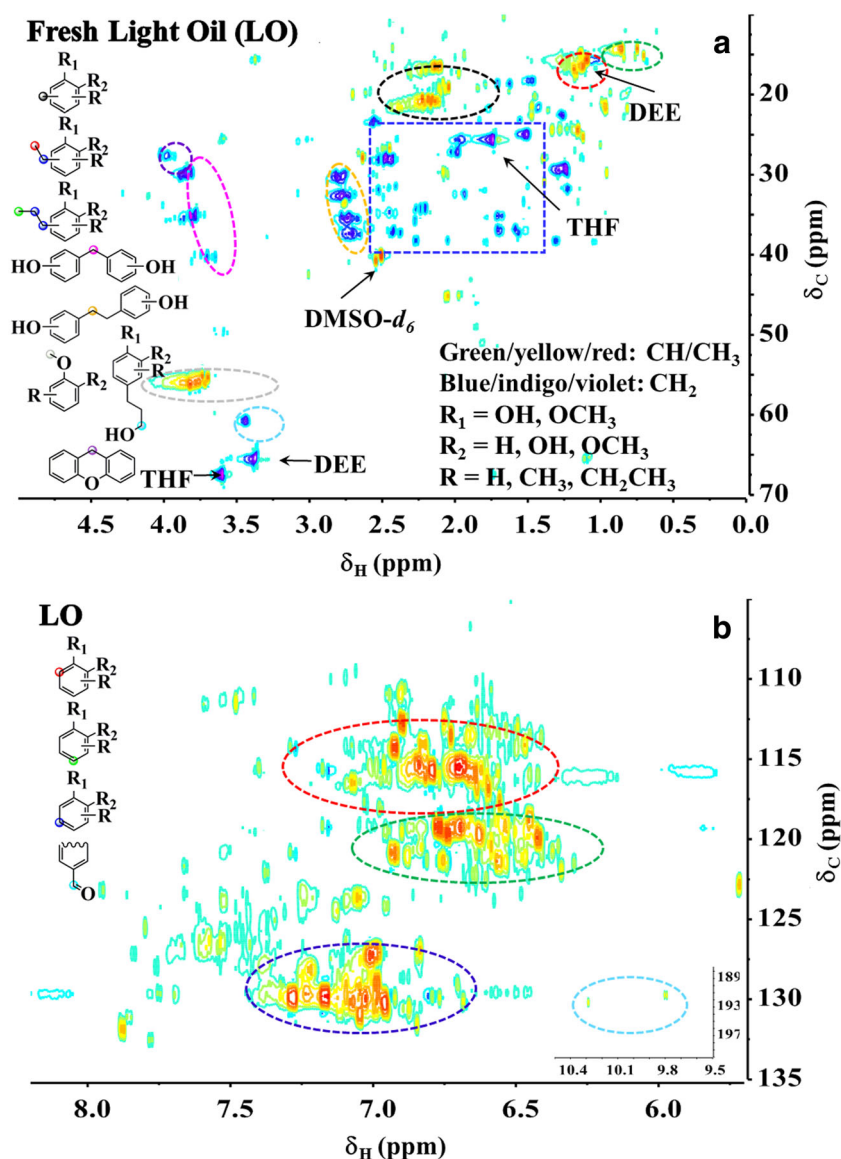
3.3.2 ¹H–¹³C HSQC NMR analysis

¹H–¹³C HSQC NMR analysis was used to confirm the structural changes that occurred during the accelerated ageing process. It allows the various structural molecules (LO, HO and THF insolubles) to be analysed irrespective of their chemical properties (i.e. volatility and Mw) and also provides a better understanding about chemical structures of all fractions of the HTL bio-oil. This analysis was facilitated by recording a new chemical-shift database of 23 model compounds in DMSO-*d*₆ (identified by GC–MS measurements) using ¹H–¹³C HSQC NMR. The results of these measurements are presented in

supplementary data (Table S1 and Fig. S1). Figure 5 shows the ¹H–¹³C HSQC NMR spectra of fresh LO. The peaks in the spectra are separated into two general regions corresponding to the aliphatic and aromatic regions. Signals corresponding to the aliphatic region, including aliphatic and ether-/non-ether-connected groups, were observed between δ_C and δ_H (10–70 and 0–5 ppm). The chemical shift region belonging to the aromatic region of the respective subunits was detected in the range of δ_C/δ_H 105–135/5.7–8.2 ppm.

The major cross-peaks in the aliphatic region of the fresh LO (Fig. 5) correspond to aromatic substituents: methylene (–CH₂–) and ethylene (–CH₂–CH₂–) groups, methoxyl

Fig. 5 Aliphatic region (δ_C/δ_H 10–70/0–5 ppm) (a) and aromatic region (δ_C/δ_H 105–135/5.7–8.2 ppm) (b) in the ^1H – ^{13}C HSQC NMR spectrum (800 MHz, $\text{DMSO}-d_6$) of the fresh light oil (LO) and the highlighted characteristic signals. *DEE* diethyl ether, *THF* tetrahydrofuran



($-\text{OCH}_3$) groups and alkyl groups (methyl ($-\text{CH}_3$), ethyl ($-\text{CH}_2-\text{CH}_3$) and propyl ($-\text{CH}_2-\text{CH}_2-\text{CH}_3$)). A notable cluster of cross-peaks at a distinct region of ^1H and ^{13}C chemical shifts is attributed to the β/γ - CH_2 groups (from an aromatic ring) adjacent to the alcohol group around δ_C/δ_H 61–65/3.4 ppm. In this study, no evidence was found for β/γ - CH_2 groups (from an aromatic ring) being present adjacent to the carboxylic groups between δ_C and δ_H (50–60 and 3.5–4.1 ppm), which is possibly due to the phase separation of the water and bio-oil outflow from the HTL reactor.

The NMR spectrum in the aromatic region of the fresh LO (Fig. 5) consists predominantly of many cross-peaks assigned to aromatic C–H bonds at the *o*-, *m*- and *p*-positions of not only phenolic rings (phenols, catechols and phenolic dimers) but also other aromatic compounds (anisoles and guaiacols). Based on the ^1H – ^{13}C HSQC NMR of the model compounds, it can be seen that the LO is dominated by phenols > anisoles,

guaiacols > catechols, and it is thus consistent with the GC–MS results. The details of the assignments are also shown in Fig. 5. These were performed based on the ^1H – ^{13}C NMR assignments of the model lignin-derived compounds in $\text{DMSO}-d_6$ and some references [26, 36–42]. These cross-peaks are related to the main types of aromatic products confirmed by GC–MS measurement.

The chemical changes in the aged LO_DEE solubles after ageing at 80 °C for 1 h, 1 day and 1 week (aLO_ES_80_1h/1d/1w) were recorded using ^1H – ^{13}C HSQC NMR and compared with the fresh LO. However, since only minor changes were detected in samples aged for 1 h and 1 day compared to the fresh sample in the ^1H – ^{13}C HSQC NMR analysis, only the 1 week spectrum of aLO_ES_80_1w was interpreted in detail. Although the use of HSQC spectra is not ideal for quantification, it is possible to observe changes in the signal intensity since all samples were prepared at the same concentration,

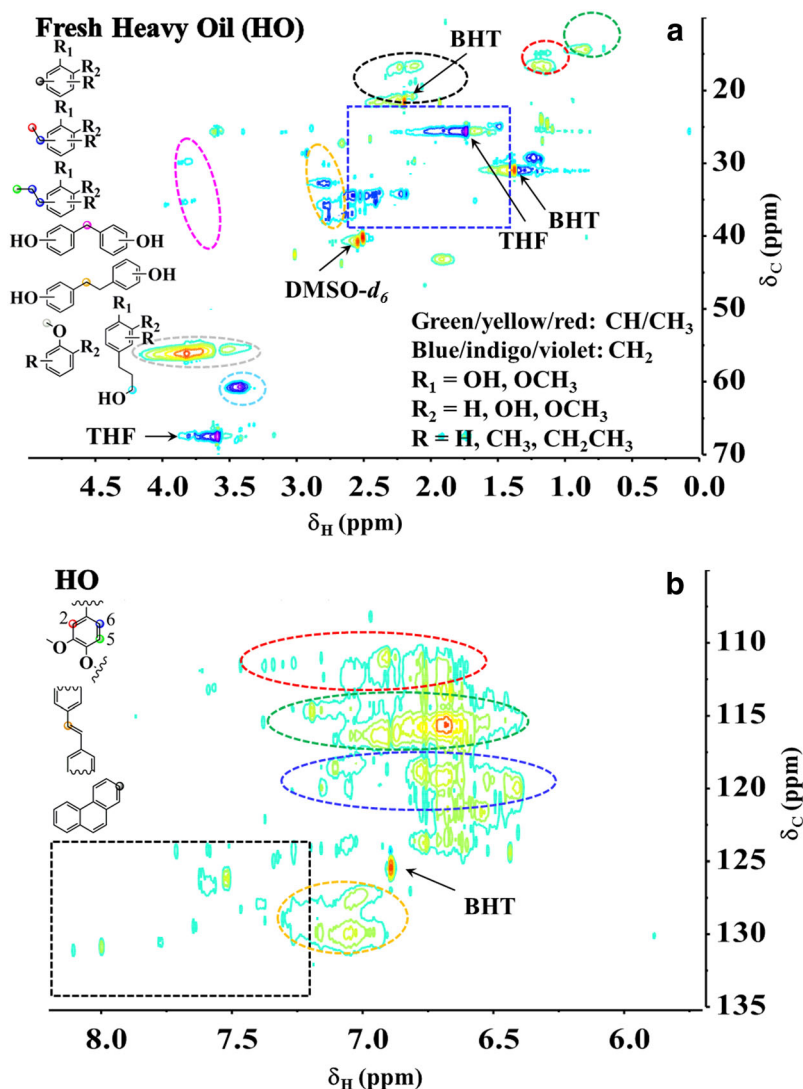
using the same solvent, and analysed at the same time [10, 19, 26]. The aliphatic and aromatic regions in the ^1H – ^{13}C HSQC NMR spectra of the LO and aged LO_DEE solubles for 1 week (aLO_ES_80_1w) are shown in Fig. S2. The pattern of functional groups is more or less the same in the fresh and aged states. Moreover, no major structural differences can be detected between the LO in either the aliphatic or aromatic regions after accelerated ageing at 80 °C for 1 week. Compared to the results of Meng et al. [14] pertaining to pyrolysis bio-oil, the LO obtained by catalytic conversion/HTL of lignin is relatively stable after ageing at 80 °C for up to 1 week.

3.4 Heavy oil

The aliphatic and aromatic regions in the ^1H – ^{13}C HSQC NMR spectra of the fresh HO are shown in Fig. 6. Unfortunately,

disturbances caused by solvent THF and the inhibitor BHT (3,5-di-*tert*-4-butylhydroxytoluene) make it difficult to interpret some areas in the aliphatic region. However, the structural motifs, such as aliphatic methylene (α/β -CH₂) and methyl ($\alpha/\beta/\gamma$ -CH₃) groups, and faint signals of methylene bridges (Ar-CH₂-Ar) can be found together with aromatic -CH (Ar2, Ar5 and Ar6), alkene bridges (Ar-CH=CH-Ar) and PAH-like structures. Although a few aliphatic dihydroconiferyl alcohol-like groups (Ar-CH₂-CH₂-CH₂-OH) still exist, none of the typical interunit linkages present in native lignin can be detected [38, 42]. The HO is generally assumed to be a macromolecule, the structure of which is mainly an aromatic network connected by alkene (vinylic and allylic-like) and aliphatic linkages (C2–C4). The components of HO are high-Mw structures, and therefore, lower signal intensity and broader peaks are obtained when they are compared with LO.

Fig. 6 Aliphatic region ($\delta_{\text{C}}/\delta_{\text{H}}$ 10–70/0–5 ppm) (a) and aromatic region ($\delta_{\text{C}}/\delta_{\text{H}}$ 105–135/5.7–8.2 ppm) (b) in the ^1H – ^{13}C HSQC NMR spectrum (800 MHz, DMSO- d_6) of the fresh heavy oil (HO) and the highlighted characteristic signals. *BHT* 3,5-di-*tert*-4-butylhydroxytoluene, *THF* tetrahydrofuran

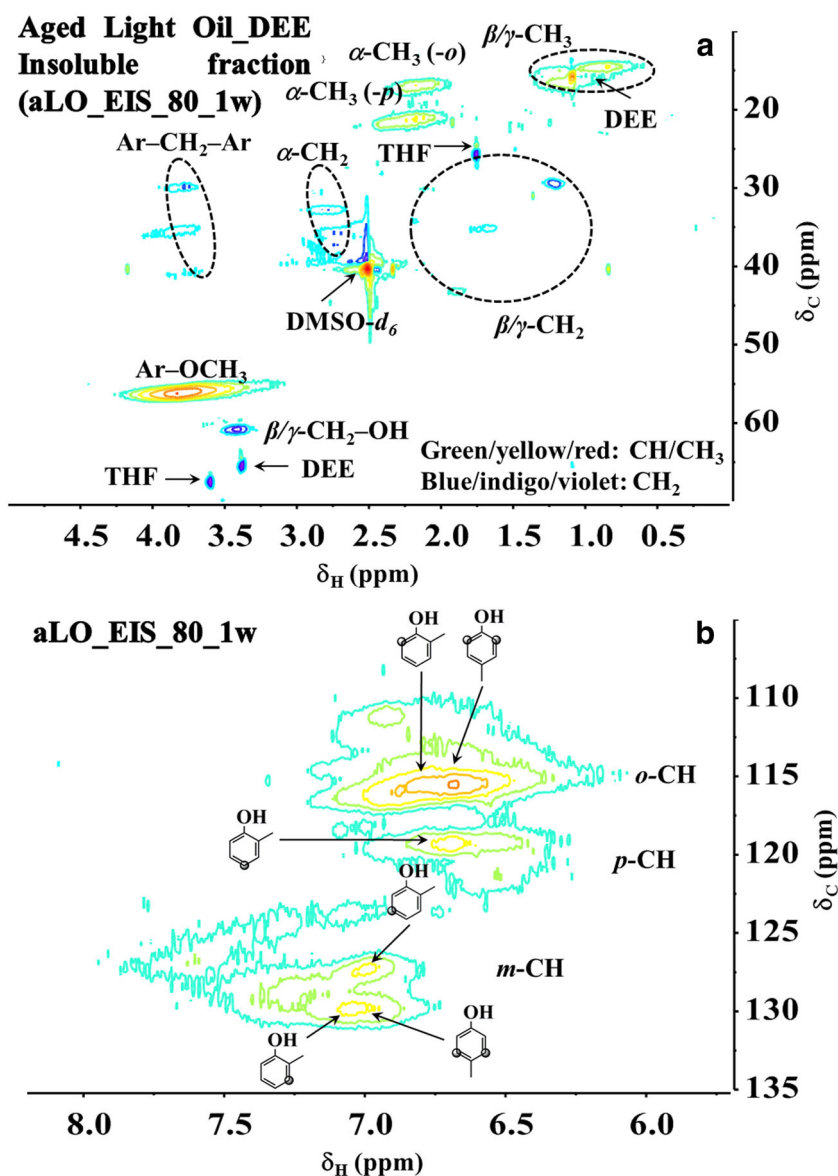


The chemical structure of the HO was analysed by applying ^1H - ^{13}C HSQC NMR to samples that were fresh (HO) and those subjected to accelerated ageing at 80 °C for 1 h, 1 day and 1 week (aHO_TS_80_1h/1d/1w). As with the LO, only minor changes in the chemical structure were detected in the 1 h and 1 day samples compared to the fresh sample, so only the 1 week spectrum of aHO_TS_80_1w was interpreted in detail. The aliphatic regions in the ^1H - ^{13}C HSQC NMR spectra of the HO at fresh state (HO) and aged state (aHO_TS_80_1w) are shown in Fig. S3. The pattern of functional groups is found to be more or less the same in both of these states for 1 week in different regions. There is, however, a minor reduction in the methyl ($-\text{CH}_3$) and methylene ($-\text{CH}_2$) groups in the ^1H - ^{13}C HSQC NMR spectrum after ageing at 80 °C for 1 week, indicating that these aliphatic structures participate in ageing reactions in the HO during

ageing at 80 °C for 1 week. There is also a decrease in the methoxyl groups in the HO, which may imply that the aromatic rings substituted by a methoxyl group are involved in the formation of heavier Mw structures in the HO after accelerated ageing. The methoxyl groups correspond to a guaiacol-like environment, as reported previously by Mattsson et al. [38], with δ_C/δ_H 56.1/3.7–3.9 ppm which is in agreement with the spectrum of the chemical-shift database of model compounds (Table S1 and Fig. S2).

Moreover, a lower intensity of cross-peaks in the aromatic region of HO ($\delta_{\text{C}}/\delta_{\text{H}}$ 114.7–116.3/6.6–6.9 ppm) after ageing at 80 °C for 1 week indicates not only a loss of aromatic C–H but also the possible formation of more C–C bonds resulting from polymerisation/condensation reactions in the oil. After ageing for 1 week, the signal cross-peaks in the guaiacol Ar2 ($\delta_{\text{C}}/\delta_{\text{H}}$ 110.7–112.4/6.6–6.9 ppm) and guaiacol Ar6 ($\delta_{\text{C}}/\delta_{\text{H}}$

Fig. 7 Aliphatic region (δ_C/δ_H 10–70/0–5 ppm) (a) and aromatic region (δ_C/δ_H 105–135/5.7–8.2 ppm) (b) in the 1H - ^{13}C HSQC NMR spectrum (800 MHz, DMSO- d_6) of the aged light oil DEE insolubles at 80 °C for 1 week (aLO_EIS_80_1w) and the highlighted characteristic signals. DEE diethyl ether, THF tetrahydrofuran, Ar aromatic ring; α -, β - and γ - corresponds to the aliphatic carbon from the aromatic ring



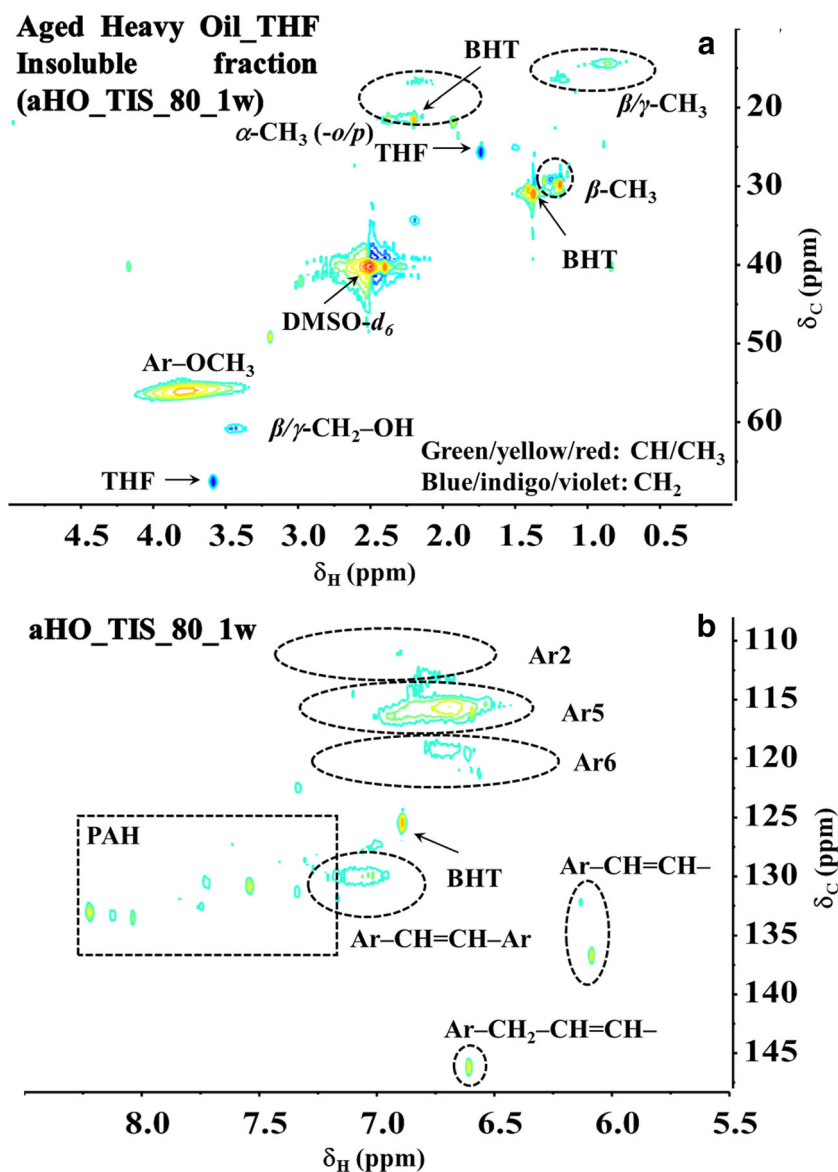
118.7–120.4/6.5–6.8 ppm) regions in ^1H – ^{13}C HSQC NMR decrease compared to those of the fresh HO: this indicates that aromatic polymerisation/condensation occurs in these positions of the guaiacol ring. The highest intensity is found in the guaiacol Ar5 region ($\delta_{\text{C}}/\delta_{\text{H}}$ 114.7–116.3/6.6–6.9 ppm), which is also where most of the other aromatic structures display cross-peaks in HSQC NMR. Ben and Ragauskas [10] revealed that the contents of all types of aromatic C–H and methoxyl bonds in the bio-oil produced from biomass-pyrolysis decreased after ageing at 80 °C for 60 h due to the condensation reactions that occurred, which support our findings. The contents of these groups (aromatic CH and methoxyl groups) decreased more rapidly in the HO than in the LO. This finding was supported by the results of the bio-oil yield, where the HO (3.1% decrease) was found to be more reactive than the LO (0.5% decrease) (see Sect. 3.1).

3.5 DEE/THF insolubles

Some small amounts of DEE/THF insolubles are formed during the ageing process, as mentioned above; they were separated from the LO/HO using DEE/THF. These aged LO_DEE insolubles (aLO_EIS_80_1w) and aged HO_THF insolubles (aHO_TIS_80_1w) were dissolved in DMSO- d_6 and investigated structurally using ^1H – ^{13}C HSQC NMR (Figs. 7 and 8).

The DEE insolubles in the aged LO (aLO_EIS_80_1w) (Fig. 7) were comprised of aromatic methyl (–CH₃), methoxyl (–OCH₃) and aliphatic methylene β/γ –CH₂ groups, as well as di-substituted aromatic methylene (–CH₂–) and ethylene (–CH₂–CH₂–) bridged structures. One cross-peak corresponding to a methylene group next to an oxygen substituent groups (β/γ –CH₂–OH/OR) was also found. In the aromatic region, the highest signal intensity of the methine (–CH) cross-peaks

Fig. 8 Aliphatic region ($\delta_{\text{C}}/\delta_{\text{H}}$ 10–70/0–5 ppm) (a) and aromatic region ($\delta_{\text{C}}/\delta_{\text{H}}$ 105–135/5.7–8.2 ppm) (b) in the ^1H – ^{13}C HSQC NMR spectrum (800 MHz, DMSO- d_6) of the aged heavy oil_THF insolubles at 80 °C for 1 week (aHO_TIS_80_1w) and the highlighted characteristic signals. BHT 3,5-di-*tert*-4-butylhydroxytoluene, THF tetrahydrofuran, Ar aromatic ring, PAH polycyclic aromatic hydrocarbon; α -, β - and γ - corresponds to the aliphatic carbon from the aromatic ring



correspond to alkylated phenolic structures at the *o*- (δ_C/δ_H 112–117/6.2–7.2 ppm), *p*- (δ_C/δ_H 117–121/6.1–7.0 ppm) and *m*- (δ_C/δ_H 127–132/6.6–7.4 ppm) positions. Altogether, the alkylated phenolic pattern in the aromatic region and the aliphatic cross-peaks found for *o/p*- aromatic methyl groups in the aliphatic region (δ_C/δ_H 16–18/1.9–2.3 ppm and 21–23/1.9–2.4 ppm) imply that alkylated phenols and phenolic dimers (Ar–CH₂–Ar) structures are to be found in this DEE insoluble polymer. This is probably a high Mw structure (char/DEE insoluble fraction) produced from small aromatic structures in the LO, such as the more reactive anisoles, guaiacols, phenols and methylene groups in the phenolic dimers (Ar–CH₂–Ar) and xanthene detected by GC–MS analysis (see Sect. 3.3.1).

In addition, the THF insolubles in the aged HO (aHO_TIS_80_1w) (Fig. 8) were found to have a similar chemical structure to that of the fresh THF insolubles (Fig. S4), with structural motifs such as aromatic CH, vinylic/allylic linkages, a PAH-like structure, branched β -methyl groups (similar to *t*Bu, *i*Pr), methoxyl groups and minor signs of aromatic and aliphatic methyl groups [38]. This indicates that the HO structures have a different origin to those of the LO. The aged HO_THF insolubles are assumed to be formed from the macromolecule structure in the HO, which has the same origin as the fresh THF insolubles, so they have a similar structural network to the fresh THF insolubles [38].

In summary, this paper has shown that although the LO has a low tendency to polymerise, some small amounts of DEE insolubles was formed after a longer storage time (1 week). It was found that these new DEE insoluble structures were different to those of the fresh HO (Mw ~5600 Da), indicating that these DEE insoluble structures were formed from the phenolic monomers in the LO. ¹H–¹³C HSQC NMR analysis showed that structures, such as *o/p*-substituted phenols (methyl, ethyl and propyl), phenolic dimers (Ar–CH₂–Ar), aromatic methoxyl substituents and aromatic rings with γ -CH₂-OH/OR, reacted during storage at 80 °C to give a new high Mw structure (DEE insolubles). This is also in good agreement with the GC–MS analysis in which the most reactive phenolic structures in the HTL LO fraction were xanthene > anisoles >> guaiacols, phenols, phenolic dimers (Ar–CH₂–Ar).

Furthermore, the HO fraction (Mw ~5600 Da) formed a THF insoluble structures (Mw ~11,000 Da) which, from a chemical perspective, was virtually identical to the THF insolubles formed in the HTL reactor (Mw ~17,000 Da). The structural network that was formed was based on an aromatic network connected by aliphatic and alkene bridges. It is plausible that the main structure of the aromatic ring is “guaiacol-like” and the condensed PAH structures with substituents are “*t*-butyl-like groups” and methyl groups. The formation of these THF insoluble structures is assumed to be driven by the reactive guaiacol-like structures that are incorporated in the fresh HO [38].

4 Conclusion

In the present work, the thermal stability of high and low Mw fractions of lignin-derived HTL bio-oil was studied. After ageing at 80 °C for 1 week, the low Mw fraction (LO) showed virtually undetectable changes in yield (from 100 to 99.5%) and molecular weight. The high Mw fraction (HO) was, however, effected slightly by ageing: the yield decreased by 3.1% during the same conditions. The high Mw insoluble fractions formed from the LO and HO were collected and analysed further using 2D HSQC NMR. It was revealed that the insolubles from the LO and HO had distinctly different structures, implying that they are of different origins (i.e. small phenolics compared to macromolecule structures). The storage stability of both the low and high Mw fractions of the HTL bio-oil was found to be remarkably high; the most reactive structures found were the aromatic rings with methoxyl groups and the phenolic dimers with a bridging methylene groups (Ar–CH₂–Ar).

Acknowledgments The authors gratefully acknowledge the financial support received from Chalmers Energy Initiative-LignoFuel Project, Valmet Power AB, The Swedish Energy Agency and Ångpanneförenings Forskningsstiftelse. Thanks go to Maxim Mayzel for help with the NMR analysis at Swedish NMR centre of Gothenburg University, to Lars-Erik Åmand for experimental support and to Tommy Friberg for technical assistance.

Open Access This article is distributed under the terms of the Creative Commons Attribution 4.0 International License (<http://creativecommons.org/licenses/by/4.0/>), which permits unrestricted use, distribution, and reproduction in any medium, provided you give appropriate credit to the original author(s) and the source, provide a link to the Creative Commons license, and indicate if changes were made.

References

- Joseph J, Rasmussen MJ, Fecteau JP, Kim S, Lee H, Tracy KA, Jensen BL, Federick BG, Stemmler EA (2016) Compositional changes to low water content bio-oils during aging: an NMR, GC/MS, and LC/MS study. *Energ Fuel* 30:4825–4840
- Chen D, Zhou J, Zhang Q, Zhu X (2014) Evaluation methods and research progresses in bio-oil storage stability. *Renew Sust Energ Rev* 40:69–79
- Hiltner RN, Das KC (2010) Comparison of three accelerated aging procedures to assess bio-oil stability. *Fuel* 89:2741–2749
- Alsibou E, Helleur B (2014) Accelerated aging of bio-oil from fast pyrolysis of hardwood. *Energ Fuel* 28:3224–3235
- Yang Z, Kumar A, Huhnke RL (2015) Review of recent developments to improve storage and transportation stability of bio-oil. *Renew Sust Energ Rev* 50:859–870
- Czernik S, Johnson DK, Black S (1994) Stability of wood fast pyrolysis oil. *Biomass Bioenerg* 7:187–192
- Boucher ME, Chaala A, Pakdel H, Roy C (2000) Bio-oils obtained by vacuum pyrolysis of softwood bark as a liquid fuel for gas turbines. Part II: stability and ageing of bio-oil and its blends with methanol and a pyrolytic aqueous phase. *Biomass Bioenerg* 19: 351–361

8. Samanya J, Hornung A, Jones M, Vale P (2011) Thermal stability of sewage sludge pyrolysis oil. *Int J Renew Energy Res* 1:66–74
9. Jiang X, Zhong Z, Ellis N, Wang Q (2011) Aging and thermal stability of the mixed product of the ether-soluble fraction of bio-oil and bio-diesel. *Chem Eng Technol* 34:727–736
10. Ben H, Ragauskas AJ (2012) In situ NMR characterization of pyrolysis oil during accelerated aging. *ChemSusChem* 5:1687–1693
11. Meng J, Moore A, Tilotta D, Kelley S, Park S (2014) Toward understanding of bio-oil aging: accelerated aging of bio-oil fractions. *ACS Sust Chem Eng* 2:2011–2018
12. Meng J, Smirnova TI, Song X, Moore A, Ren X, Kelley S, Parka S, Tilotta D (2014) Identification of free radicals in pyrolysis oil and their impact on bio-oil stability. *RSC Adv* 4:29840–22846
13. Garcia-Pérez M, Chaala A, Pakdel H, Kretschmer D, Rodrigue D, Roy C (2006) Evaluation of the influence of stainless steel and copper on the aging process of bio-oil. *Energy Fuel* 20:786–795
14. Meng J, Moore A, Tilotta DC, Kelley SS, Adhikari S, Park S (2015) Thermal and storage stability of bio-oil from pyrolysis of torrefied wood. *Energy Fuel* 29:5117–5126
15. Li H, Xia S, Li Y, Ma P, Zhao C (2015) Stability evaluation of fast pyrolysis oil from rice straw. *Chem Eng Sci* 135:258–265
16. Chaala A, Ba T, Garcia-Pérez M, Roy C (2004) Colloidal properties of bio-oils obtained by vacuum pyrolysis of softwood bark: aging and thermal stability. *Energy Fuel* 18:1535–1542
17. Oasmaa A, Fonts I, Pelaez-Samaniego MR, Garcia-Perez ME, Garcia-Perez M (2016) Pyrolysis oil multiphase behaviour and phase stability: a review. *Energy Fuel* 30:6179–6200
18. Adjaye JD, Sharma RK, Bakhshi NN (1992) Characterization and stability analysis of wood-derived bio-oil. *Fuel Process Technol* 31: 241–256
19. Salanti A, Zoia L, Orlandi M, Zanini F, Elegir G (2010) Structural characterization and antioxidant activity evaluation of lignins from rice husk. *J Agr Food Chem* 58:10049–10055
20. Nguyen Lyckeskog H, Mattsson C, Åmand L-E, Olausson L, Andersson S-I, Vamling L, Theliander H (2016) Storage stability of bio-oils derived from the catalytic conversion of softwood Kraft lignin in subcritical water. *Energy Fuel* 30:3097–3106
21. Nguyen TDH, Maschietti M, Belkheiri T, Åmand L-E, Theliander H, Vamling L, Olausson L, Andersson S-I (2014) Catalytic depolymerisation and conversion of Kraft lignin into liquid products using near-critical water. *J Supercrit Fluid* 86:67–75
22. Nguyen TDH, Maschietti M, Åmand L-E, Vamling L, Olausson L, Andersson S-I, Theliander H (2014) The effect of temperature on the catalytic conversion of Kraft lignin using near-critical water. *Bioresour Technol* 170:196–203
23. Belkheiri T, Vamling L, Nguyen TDH, Maschietti M, Olausson L, Andersson S-I, Åmand L-E, Theliander H (2014) Kraft lignin depolymerization in near-critical water: effect of changing co-solvent. *Cell Chem Technol* 48:813–818
24. Belkheiri T, Mattsson C, Andersson S-I, Olausson L, Åmand L-E, Theliander H, Vamling L (2016) Effect of pH on Kraft lignin depolymerisation in subcritical water. *Energy Fuel* 30:4916–4924
25. Elliott DC, Oasmaa A, Meier D, Preto F, Bridgwater AV (2012) Results of the IEA round robin on viscosity and aging of fast pyrolysis bio-oils: long-term tests and repeatability. *Energy Fuel* 26: 7362–7366
26. Ben H, Ragauskas AJ (2011) Heteronuclear single-quantum correlation–nuclear magnetic resonance (HSQC–NMR) fingerprint analysis of pyrolysis oils. *Energy Fuel* 25:5791–5801
27. Johns IB, McElhill EA, Smith JO (1962) Thermal stability of some organic compounds. *J Chem Eng Data* 7:277–281
28. Wright JS, Shadnia H, Chepelev LL (2009) Stability of carbon-centered radicals: effect of functional groups on the energetics of addition of molecular oxygen. *J Comput Chem* 30:1016–1026
29. Yangfei C, Zhiqin C, Shaoyi X, Hongbo L (2008) A novel thermal degradation mechanism of phenol-formaldehyde type resins. *Thermochim Acta* 476:39–43
30. Chanyshv AD, Litasov KD, Shatskiy AF, Ohtani E (2014) Study of pycyclic aromatic hydrocarbons at a pressure of 6–9 GPa with X-ray diffraction and synchrotron radiation. *Dokl Earth Sci* 458:1277–1280
31. Fiege H (2000) Cresols and xylenols. In: Ullmann's encyclopedia of industrial chemistry, 7th edn. Wiley, New York
32. Fiege H, Voges H-W, Hamamoto T, Umemura S, Iwata T, Miki H, Fujita Y, Buysch H-J, Garbe D, Paulus W (2000) Phenol derivatives. In: Ullmann's encyclopedia of industrial chemistry, 7th edn. Wiley, New York
33. Li J-K, Huang X-Q, Yang S, Ma H-W, Chi Y-N, Hu C-W (2015) Four alkoxyhexavanadate-based Pd-polyoxovanadates as robust heterogeneous catalysts for oxidation of benzyl-alkanes. *Inorg Chem* 54:1454–1461
34. Weber M, Weber M, Kleine-Boymann M (2000) Phenol. In: Ullmann's encyclopedia of industrial chemistry, 7th edn. Wiley, New York
35. Schmidt R, Griesbaum K, Behr A, Biedenapp D, Voges H-W, Garbe D, Paetz C, Collin G, Mayer D, Höke H (2000) Hydrocarbons. In: Ullmann's encyclopedia of industrial chemistry, 7th edn. Wiley, New York
36. Giummarella N, Zhang L, Henriksson G, Lawoko M (2016) Structural features of mildly fractionated lignin carbohydrate complexes (LCC) from spruce. *RSC Adv* 6:42120–42131
37. Huang X, Korányi TI, Boot MD, Hensen EJM (2015) Ethanol as capping agent and formaldehyde scavenger for efficient depolymerization of lignin to aromatics. *Green Chem* 17:4941–4950
38. Mattsson C, Andersson S-I, Belkheiri T, Åmand L-E, Olausson L, Vamling L, Theliander H (2016) Using 2D NMR to characterize the structure of the low and high molecular weight fractions of bio-oil obtained from LignoBoost™ Kraft lignin depolymerized in subcritical water. *Biomass Bioenerg*. doi:10.1016/j.biombioe.2016.09.004
39. Sudasinghe N, Cort JR, Hallen R, Olarte M, Schmidt A, Schaub T (2014) Hydrothermal liquefaction oil and hydrotreated product from pine feedstock characterized by heteronuclear two-dimensional NMR spectroscopy and FT-ICR mass spectrometry. *Fuel* 137:60–69
40. Narani A, Chowdari RK, Cannilla C, Bonura G, Frusteri F, Heeres HJ, Barta K (2015) Efficient catalytic hydrotreatment of Kraft lignin to alkylphenolics using supported NiW and NiMo catalysts in supercritical methanol. *Green Chem* 17:5046–5057
41. Yue F, Lu F, Ralph S, Ralph J (2016) Identification of 4–O–5-units in softwood lignins via definitive lignin models and NMR. *Biomacromolecules* 17:1909–1920
42. Constant S, Wienk HLJ, Frissen AE, Peinder P, Boelens R, Es DS, Grisel RJH, Weckhuysen BM, Huijgen WJJ, Gosselink RJA, Bruijninx PCA (2016) New insights into the structure and composition of technical lignins: a comparative characterisation study. *Green Chem* 18:2651–2665